

High Throughput Scanning of Dimer Interactions Facilitating to Confirm Molecular Stacking Mode: A Case of 1, 3, 5-Trinitrobenzene and Its Amino-derivatives

Xudong He,[†] Ying Xing,[†] Xianfeng Wei,[‡] and Chaoyang Zhang^{*†,§}

[†]*Institute of Chemical Materials, China Academy of Engineering Physics (CAEP), P. O. Box 919-311, Mianyang, Sichuan 621900, China.*

[‡]*Co-Innovation Center for NewEnergetic Materials, Southwest University of Science and Technology, Mianyang, Sichuan 621010, China.*

[§]*Beijing Computational Science Research Center, Beijing 100048, China.*

Supporting Information (SI)

Table of Contents

S1: Models for sequential and concurrency computations and workflow of high throughput computations.

S2: PES scanning of the coplanar stacking.

S3: PES scanning of the parallel stacking.

S4: PES scanning of the T-or V-shaped stacking.

S5: PES scanning of the crossing stacking.

S6: Summary of the locally lowest points on all PESs and the related ΔE_{int} .

S1: Models for sequential and concurrency computations and workflow of high throughput computations.

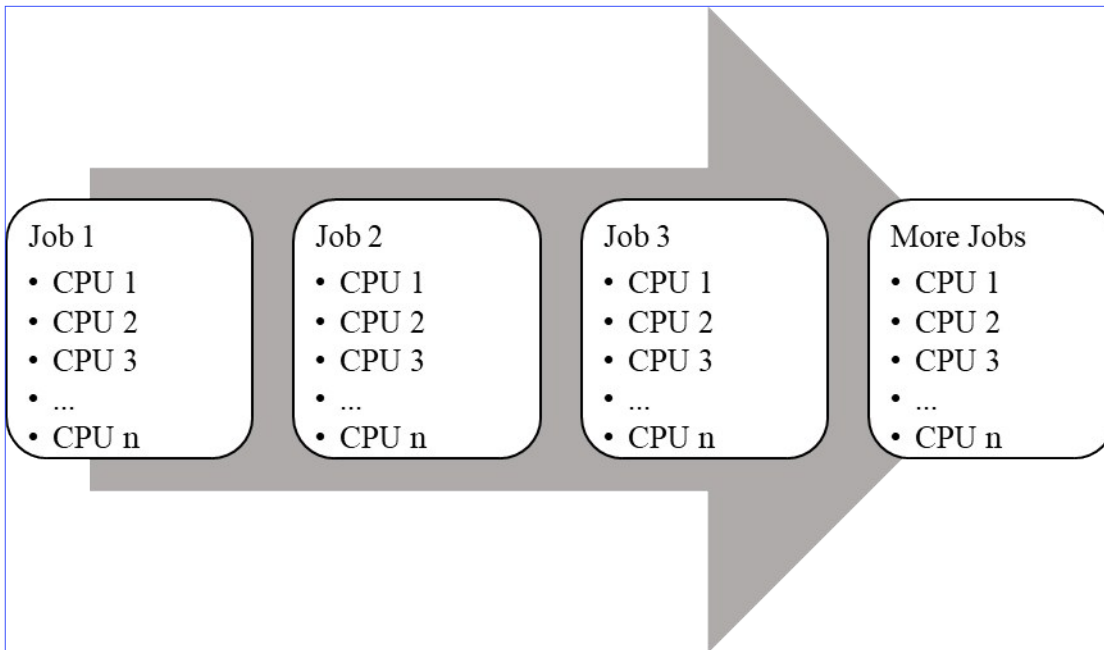


Figure S1. Model for sequential computations.

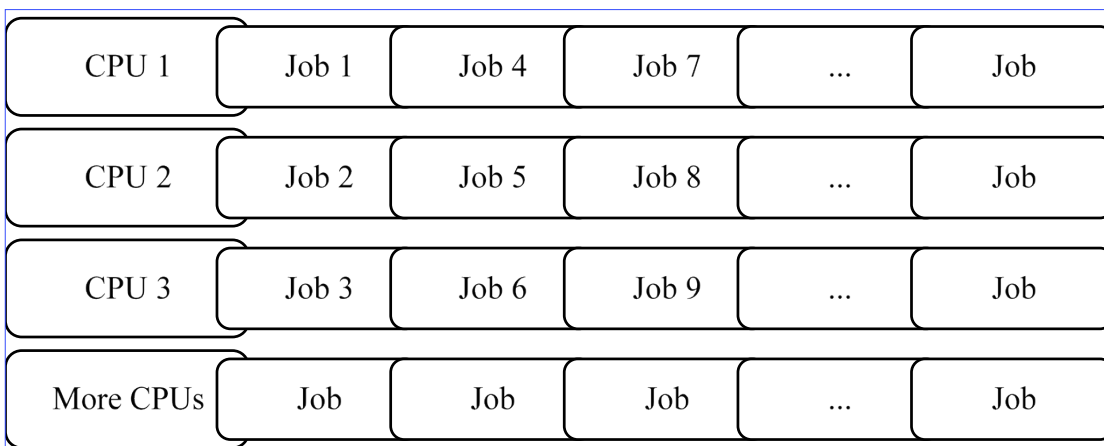


Figure S2. Model for concurrency computations.

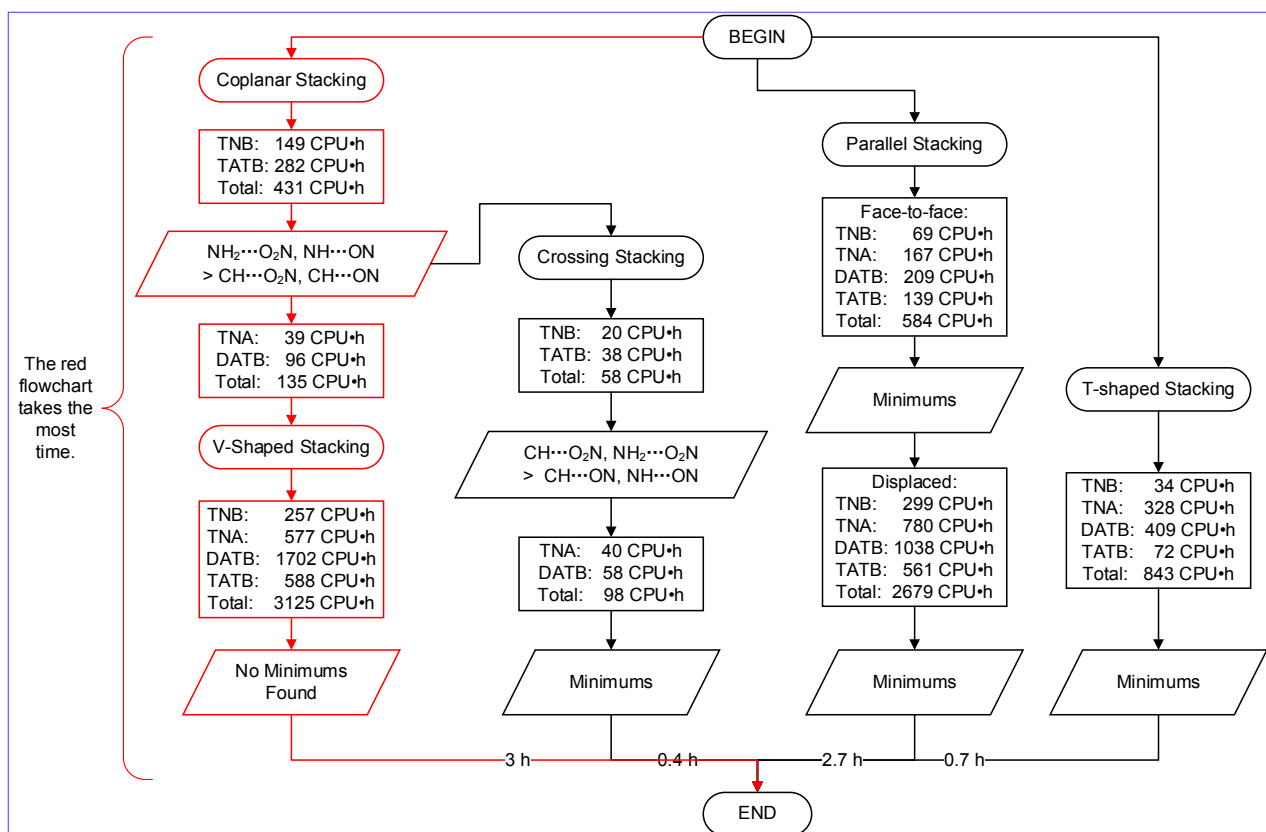


Figure S3. Workflow of high throughput computations.

S2: PES scanning of the coplanar stacking.

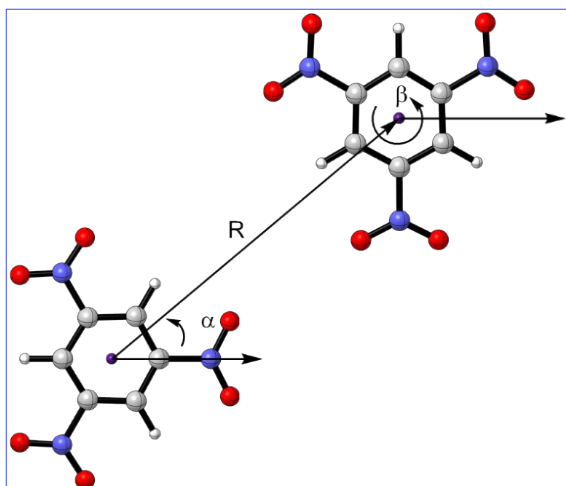


Figure S4. Freedom degrees in the case of coplanar stacking.

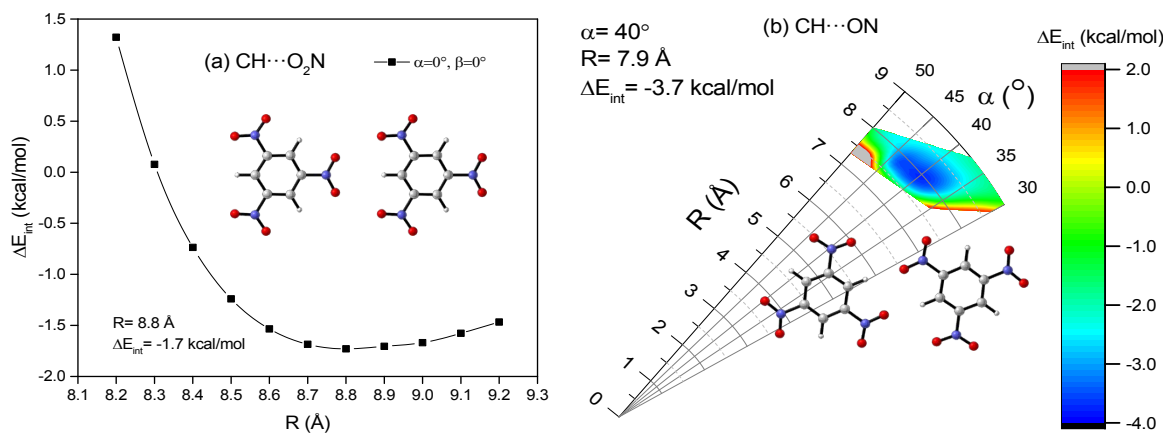


Figure S5. PESs of the coplanar TNB dimers.

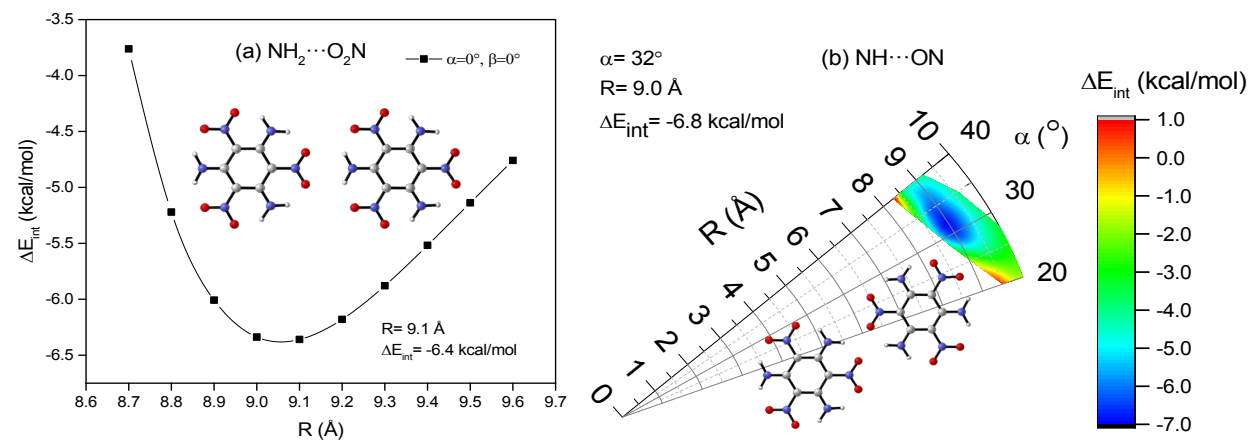


Figure S6. PESs of the coplanar TATB dimers.

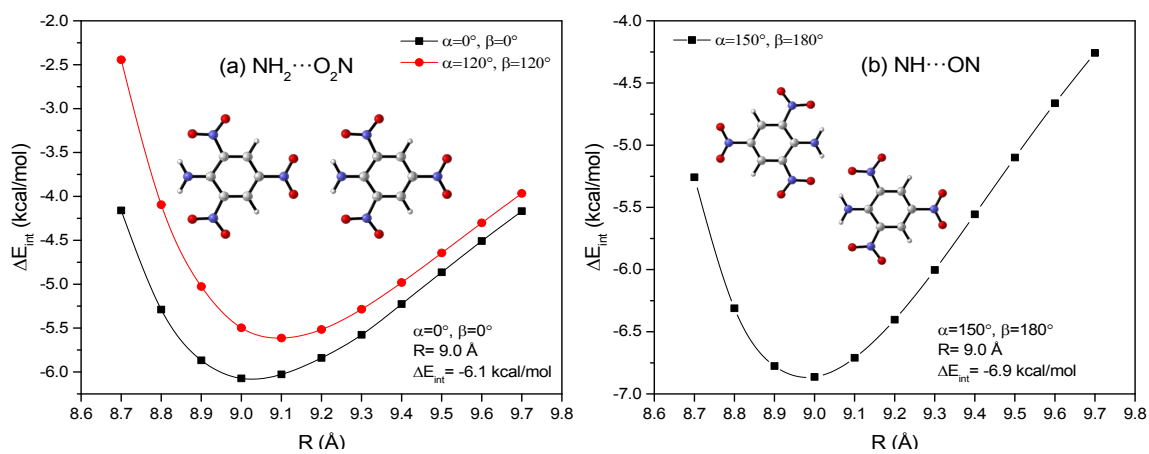


Figure S7. PESs of the coplanar TNA dimers.

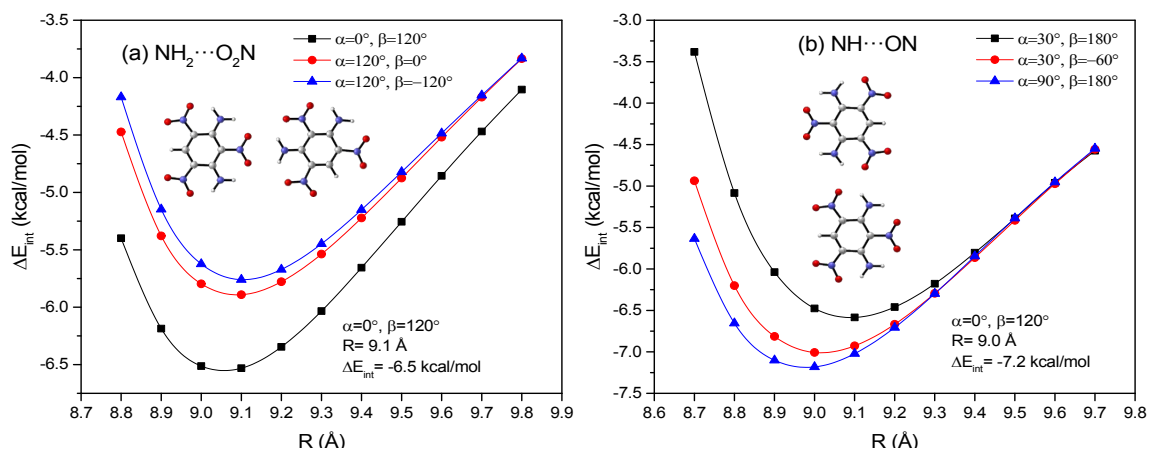


Figure S8. PESs of the coplanar DATB dimers.

S3: PES scanning of the parallel stacking.

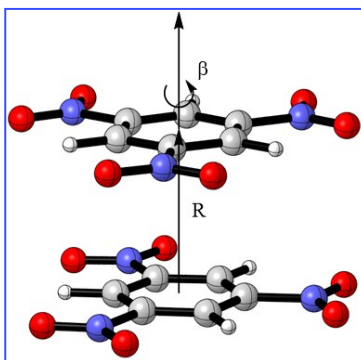


Figure S9. Plot showing the face-to-face stacking.

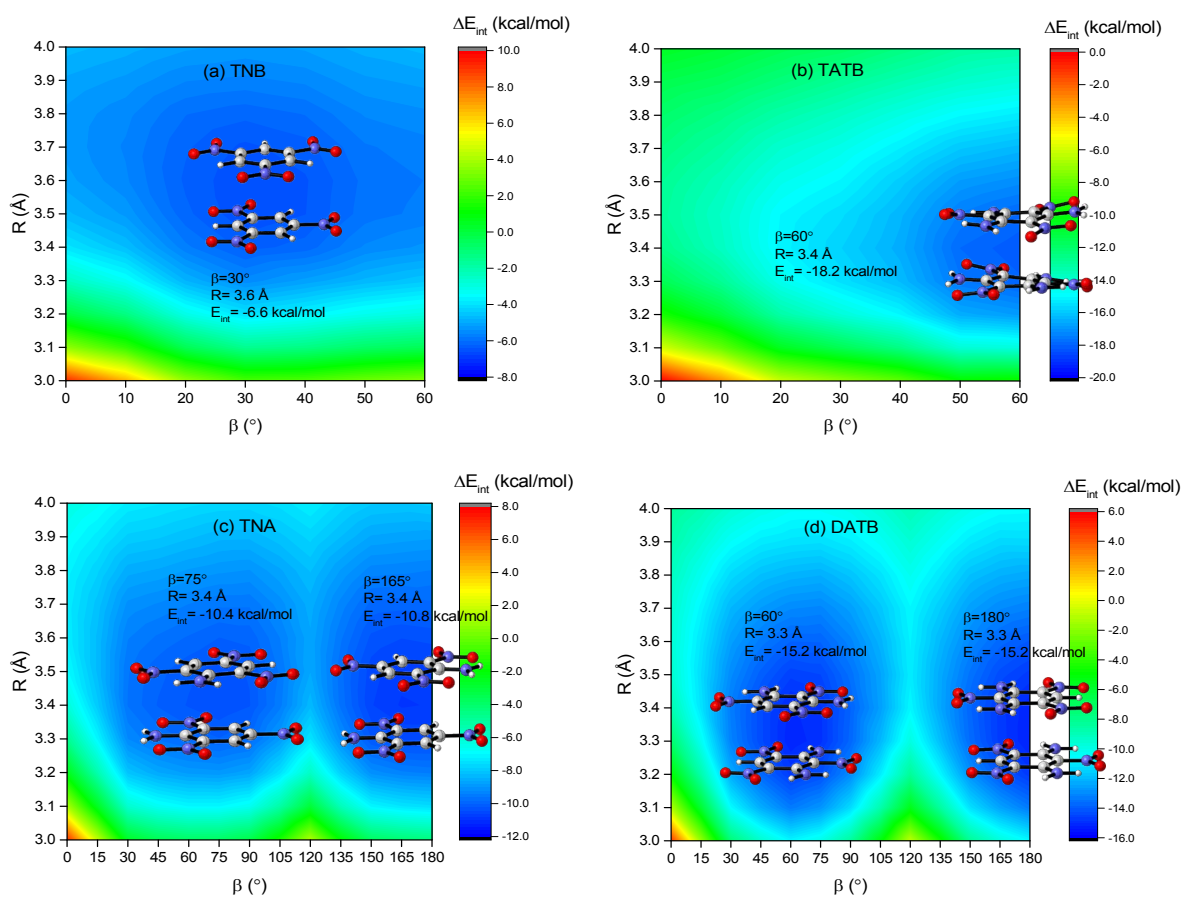


Figure S10. PESs of the face-to-face stacked dimers of the four interested molecules.

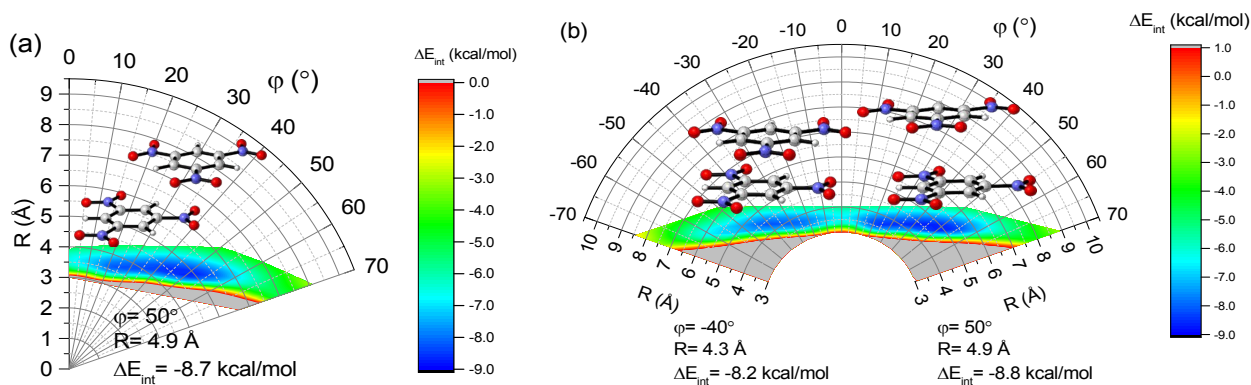


Figure S11. PESs of the parallel TNB dimers at (a) $\beta_0=30^\circ$ and $\alpha=15^\circ$ and (b) $\beta_0=30^\circ$ and $\alpha=105^\circ$.

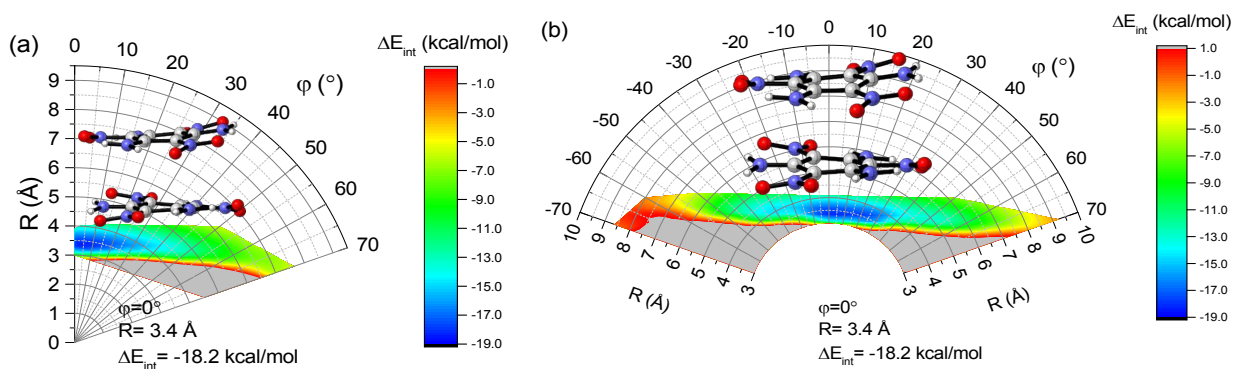


Figure S12. PESs of the parallel TATB dimers at (a) $\beta_0=60^\circ$ and $\alpha=30^\circ$ and (b) $\beta_0=60^\circ$ and $\alpha=120^\circ$.

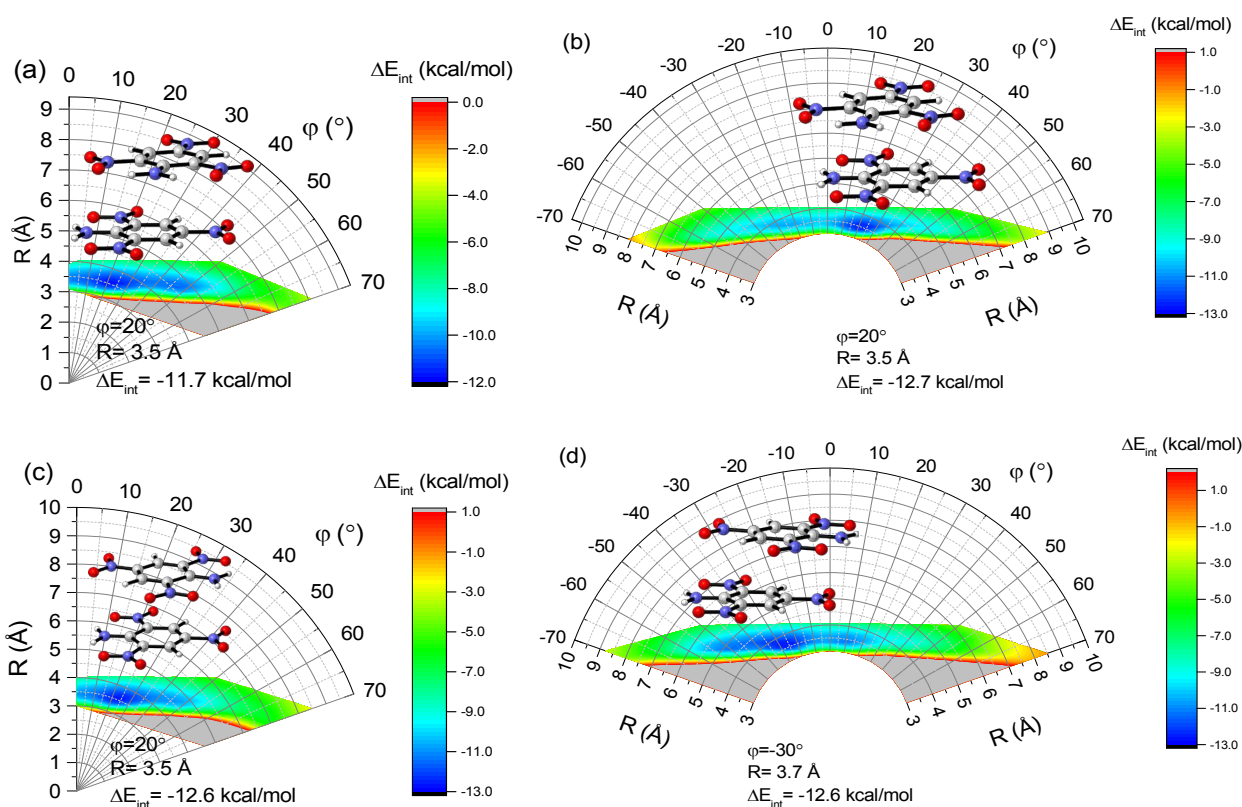


Figure S13. PESs of the parallel TNA dimers at (a) $\beta_0=75^\circ$ and $\alpha=37.5^\circ$, (b) $\beta_0=75^\circ$ and $\alpha=127.5^\circ$, (c) $\beta_0=165^\circ$ and $\alpha=82.5^\circ$ and (d) $\beta_0=165^\circ$ and $\alpha=172.5^\circ$.

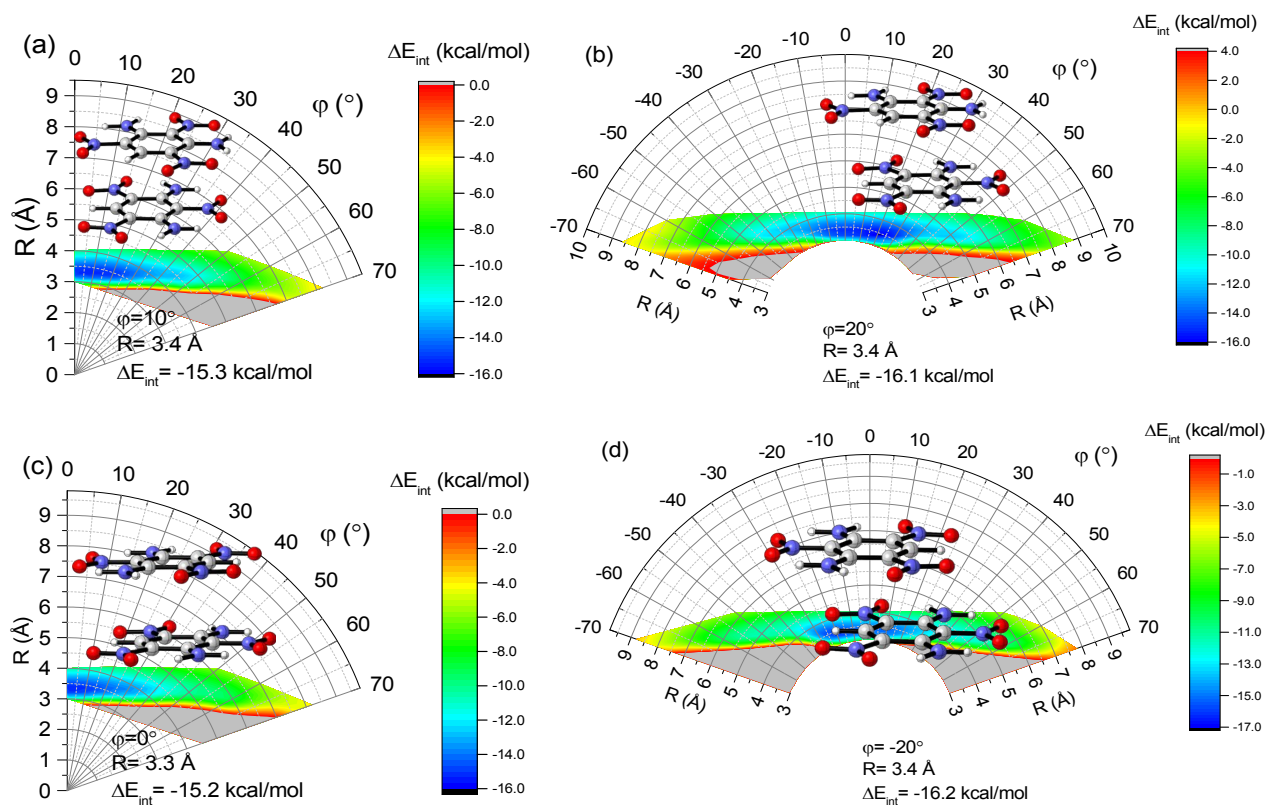


Figure S14. PESs of the parallel DATB dimers at (a) $\beta_0=60^\circ$ and $\alpha=30^\circ$, (b) $\beta_0=60^\circ$ and $\alpha=120^\circ$, (c) $\beta_0=165^\circ$ and $\alpha=172.5^\circ$, and (d) $\beta_0=165^\circ$ and $\alpha=172.5^\circ$.

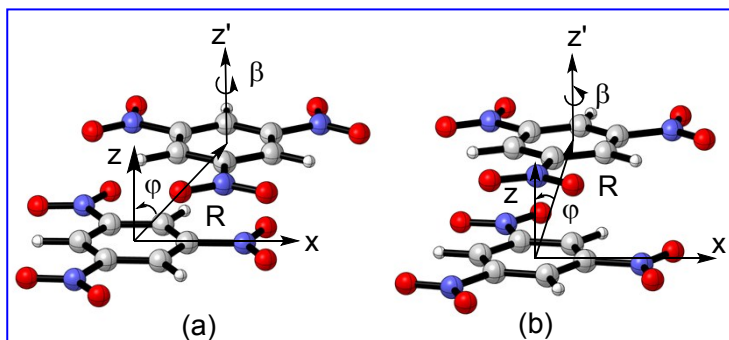


Figure S15. Two orientations of offset parallel stacking: along internal (a) and external (b) angle bisectors.

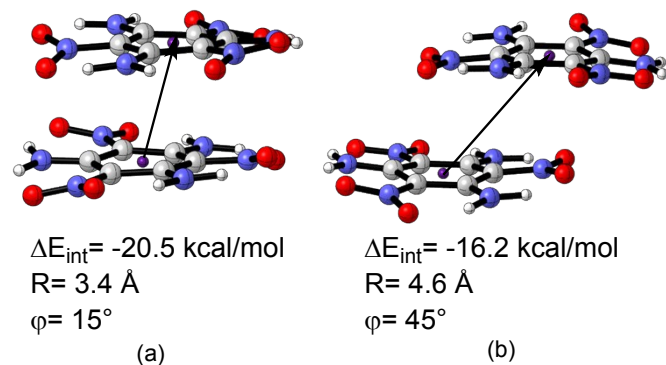


Figure S16. Configurations of the locally lowest points on PESs and the corresponding ΔE_{int} of face-to-face stacked dimers of TATB from the full optimization from a complete face-to-face stacking (a) and stacking observed in crystal (b).

S4: PES scanning of the T-or V-shaped stacking.

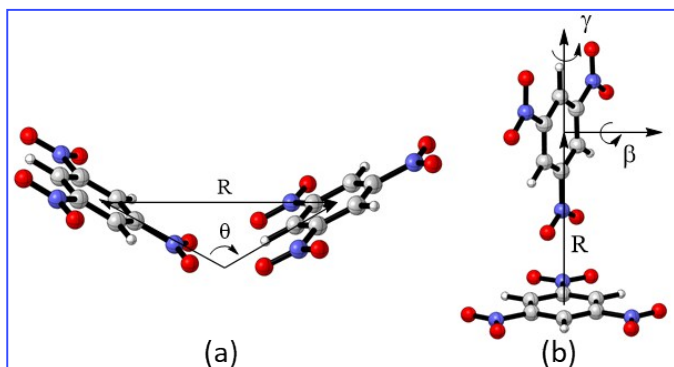


Figure S17. Variables in V- and T-shaped stacking.

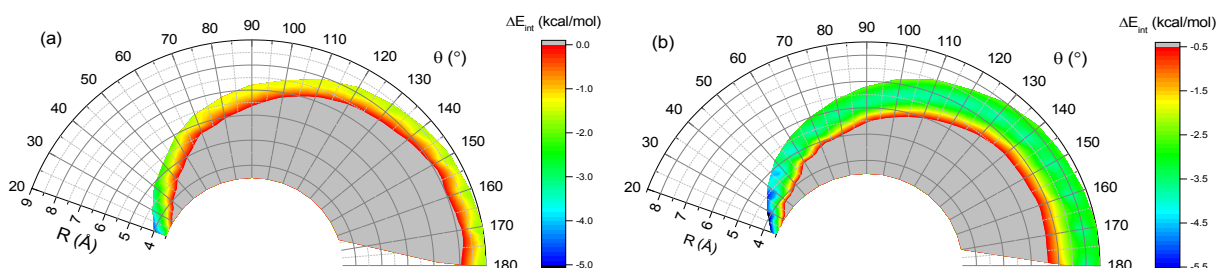


Figure S18. PESs of the V-shaped TNB dimers at (a) $\alpha=0^\circ$ and $\beta=60^\circ$ and (b) $\alpha=40^\circ$ and $\beta=40^\circ$.

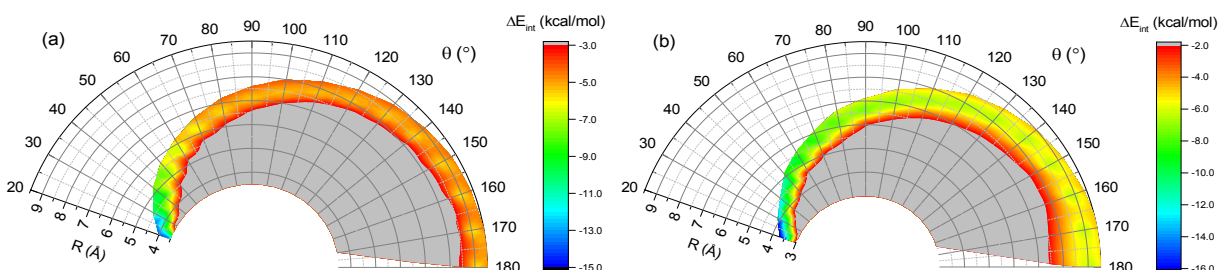


Figure S19. PESs of V-shaped TATB dimers at (a) $\alpha=0^\circ$ and $\beta=60^\circ$ and (b) $\alpha=30^\circ$ and $\beta=30^\circ$.

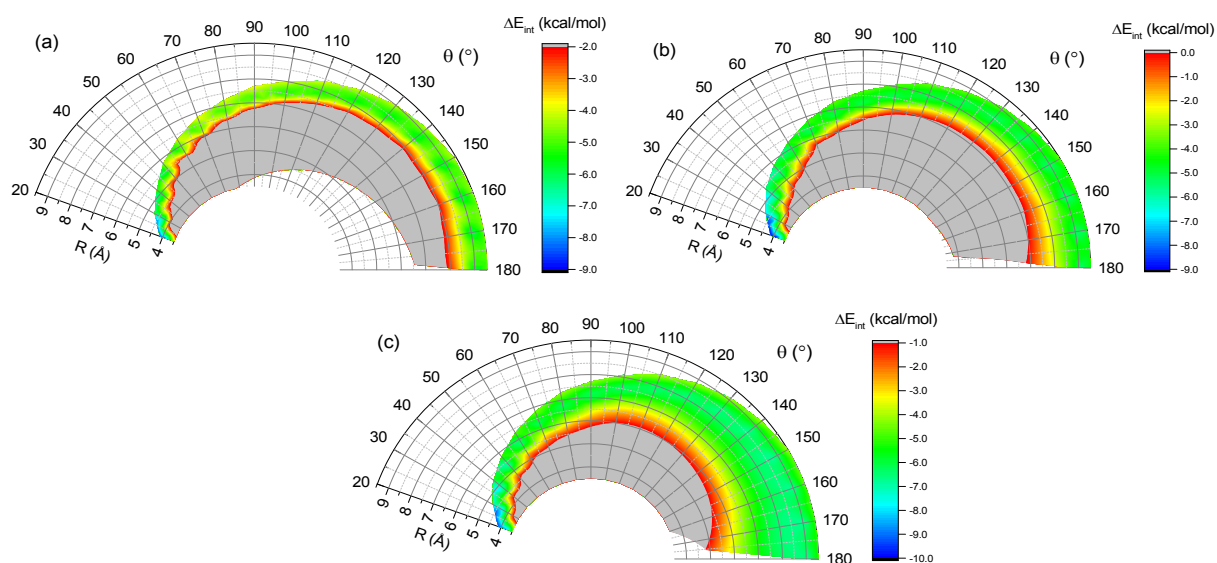


Figure S20. PESs of the V-shaped TNA dimers at (a) $\alpha=0^\circ$ and $\beta=180^\circ$, (b) $\alpha=120^\circ$ and $\beta=180^\circ$, and (c) $\alpha=150^\circ$ and $\beta=150^\circ$.

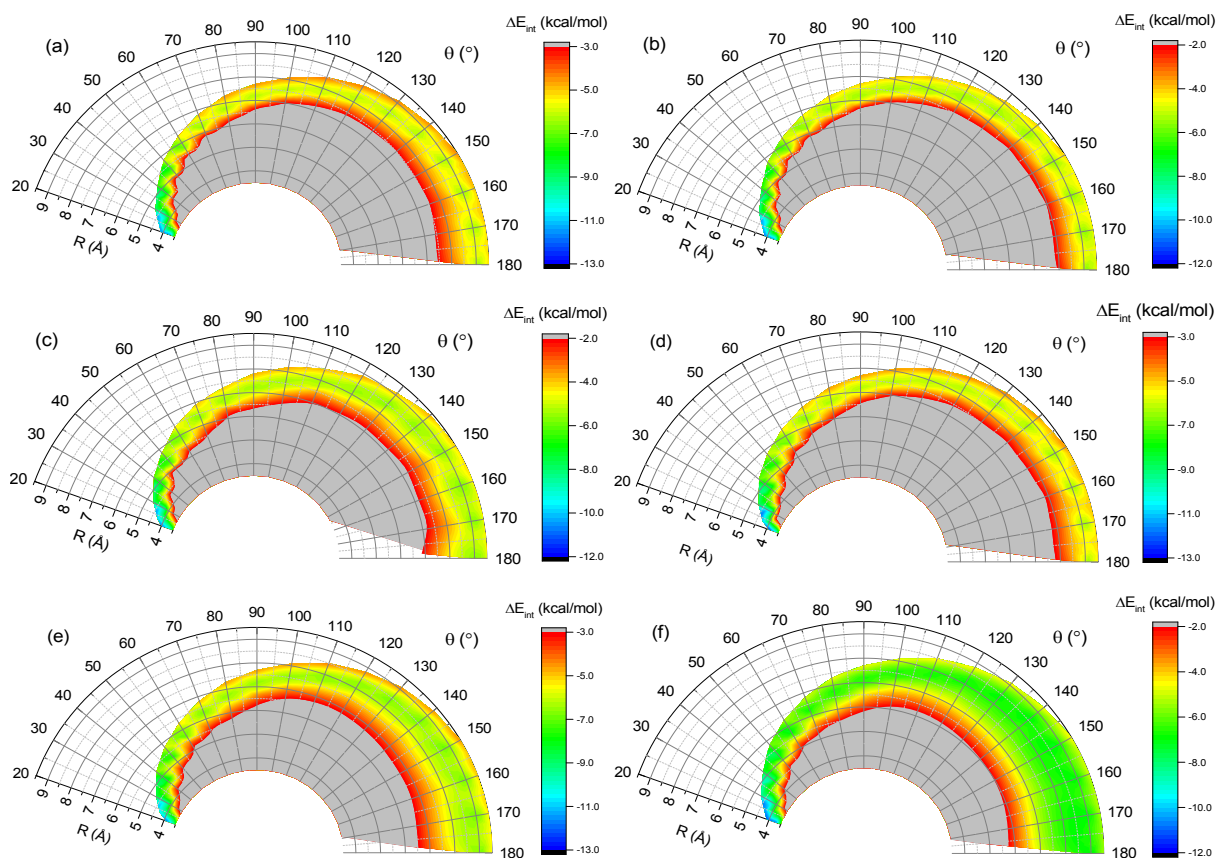


Figure S21. PESs of the V-shaped DATB dimers at (a) $\alpha=0^\circ$ and $\beta=60^\circ$, (b) $\alpha=120^\circ$ and $\beta=60^\circ$, (c) $\alpha=120^\circ$ and $\beta=-60^\circ$, (d) $\alpha=30^\circ$ and $\beta=30^\circ$, (e) $\alpha=30^\circ$ and $\beta=-90^\circ$, and (f) $\alpha=90^\circ$, $\beta=90^\circ$.

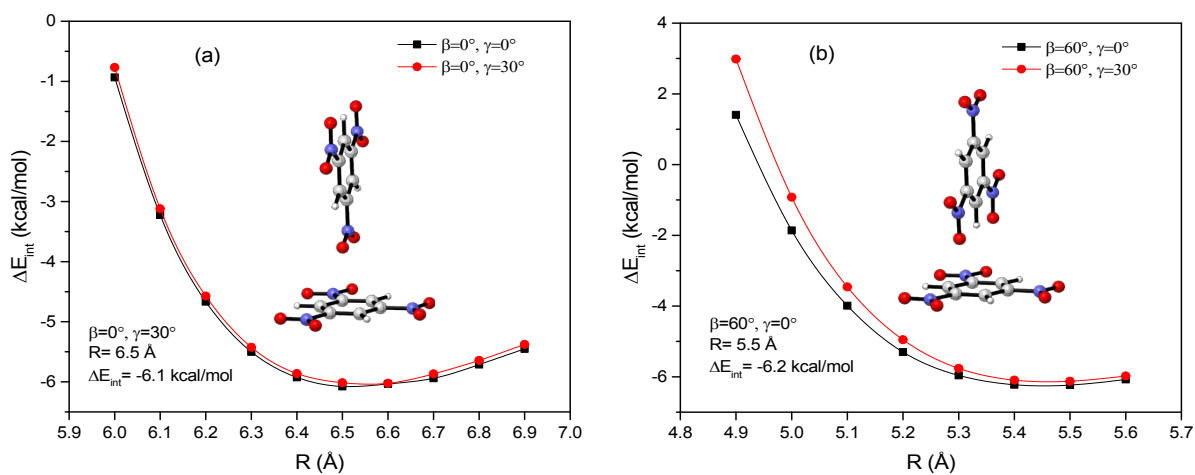


Figure S22. PESs of the T-shaped TNB dimers stacked along (a) $\text{NO}_2 \cdots \text{C}_6$ and (b) $\text{CH} \cdots \text{C}_6$.

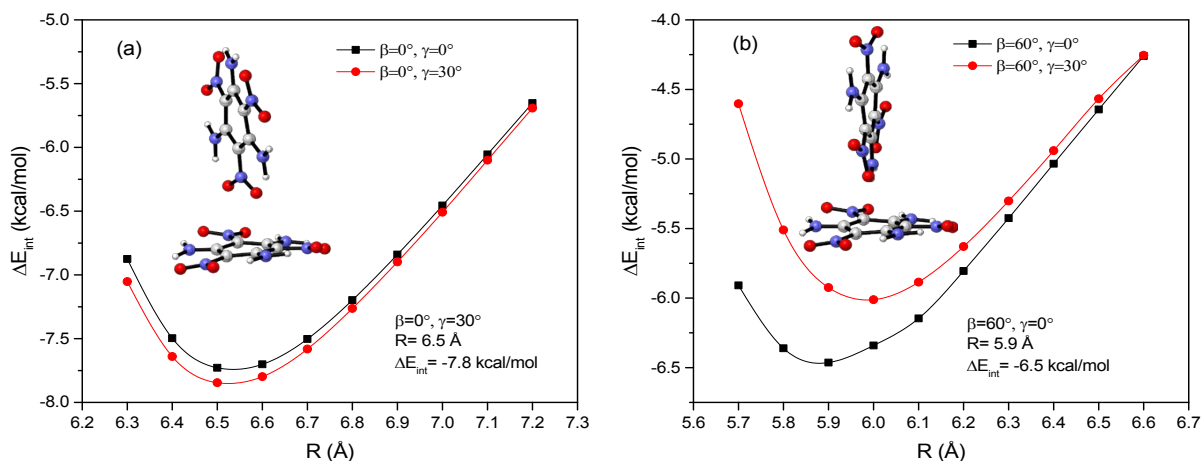


Figure S23. PESs of the T-shaped TATB dimers along (a) $\text{NO}_2 \cdots \text{C}_6$ and (b) $\text{NH}_2 \cdots \text{C}_6$.

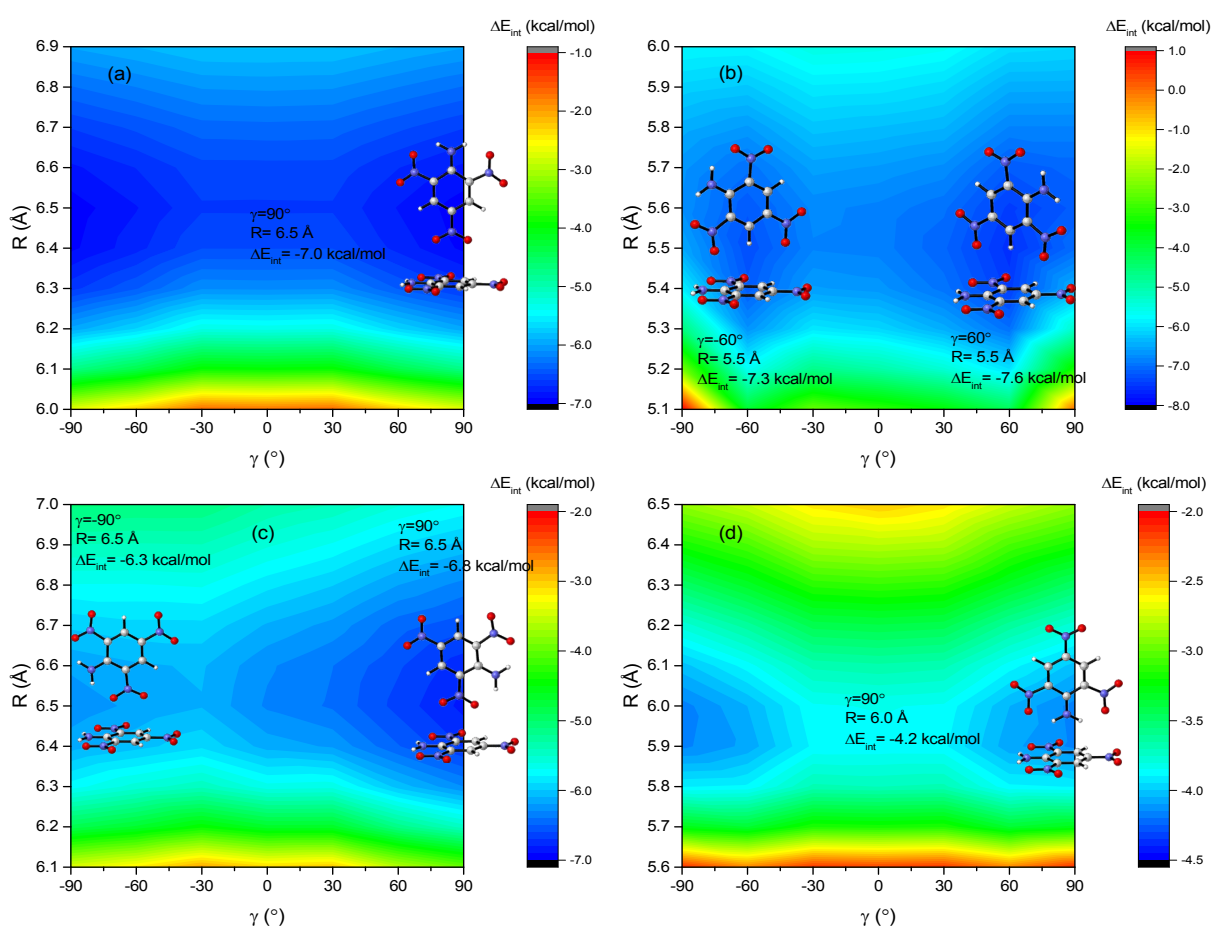


Figure S24. PESs of T-shaped TNA dimers along (a) $\text{NO}_2 \cdots \text{C}_6$, (b) $\text{CH} \cdots \text{C}_6$, (c) $\text{NO}_2 \cdots \text{C}_6$, and (d) $\text{NH}_2 \cdots \text{C}_6$.

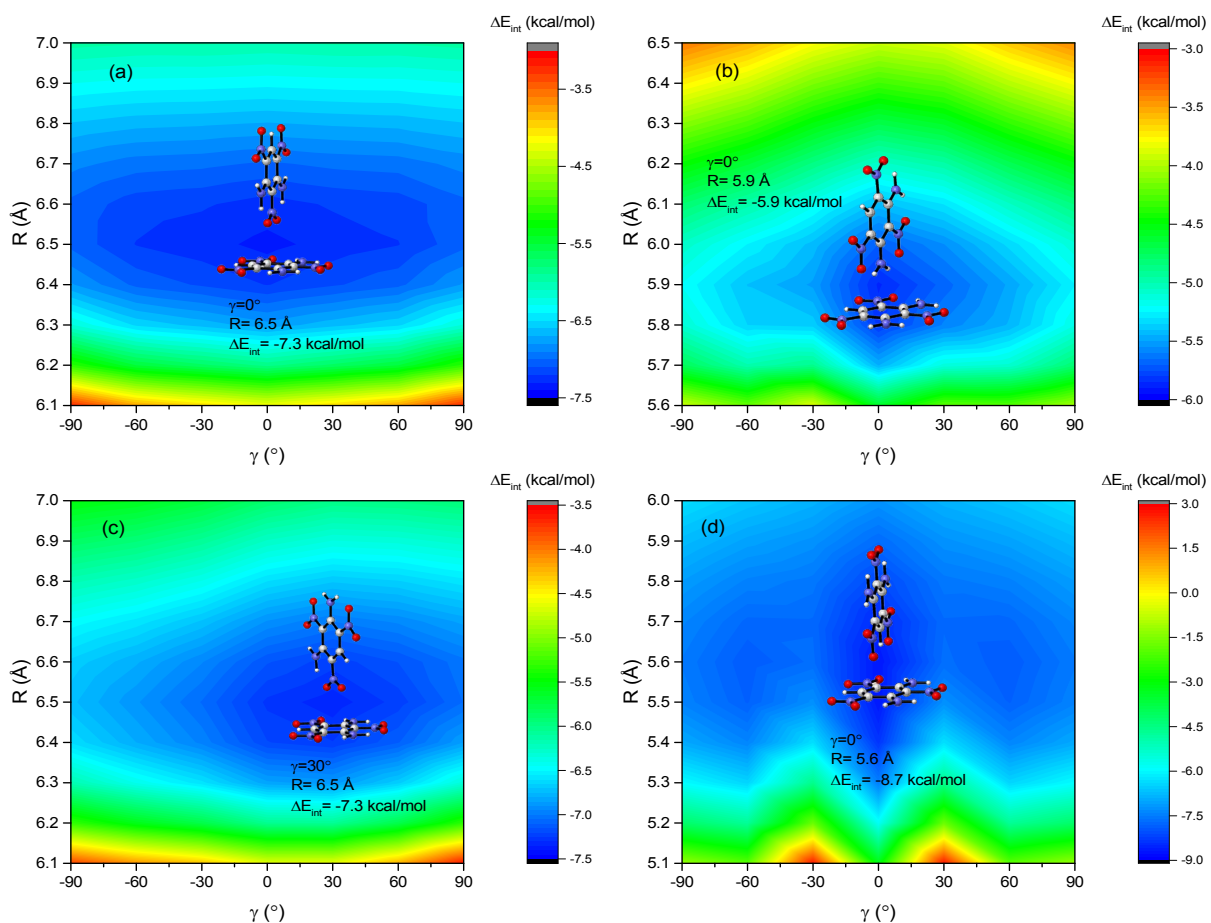


Figure S25. PESs of T-shaped DATB dimers along (a) $\text{NO}_2 \cdots \text{C}_6$, (b) $\text{NH}_2 \cdots \text{C}_6$, (c) $\text{NO}_2 \cdots \text{C}_6$, and (d) $\text{CH} \cdots \text{C}_6$.

S5: PES scanning of the crossing stacking.

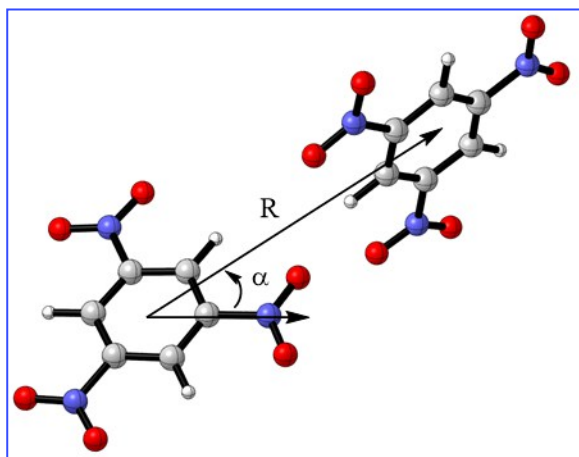


Figure S26. Degree of freedom of crossing stacking.

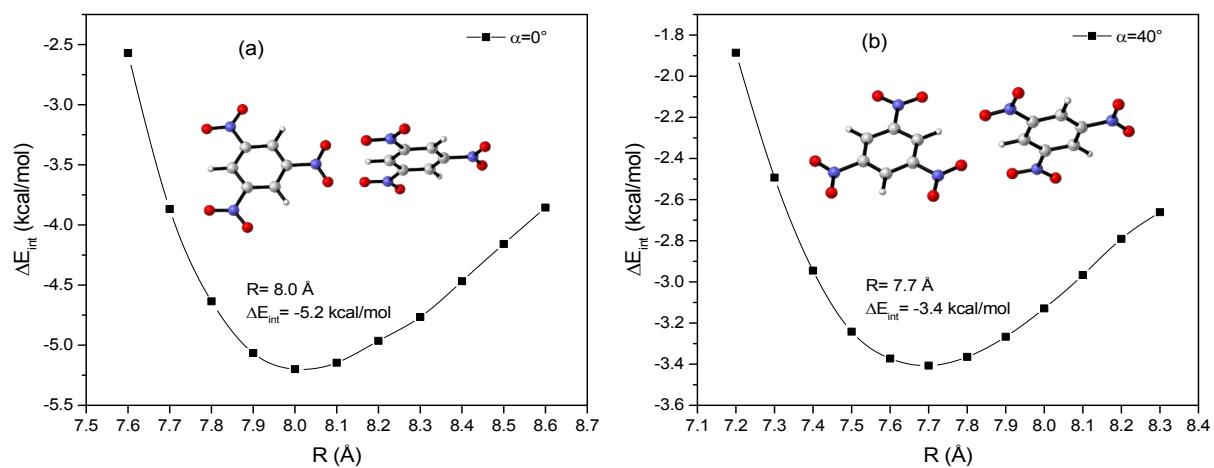


Figure S27. PESs of the crossing TNB dimers along (a) $\text{CH}\cdots\text{NO}_2$ and (b) $\text{CH}\cdots\text{NO}$.

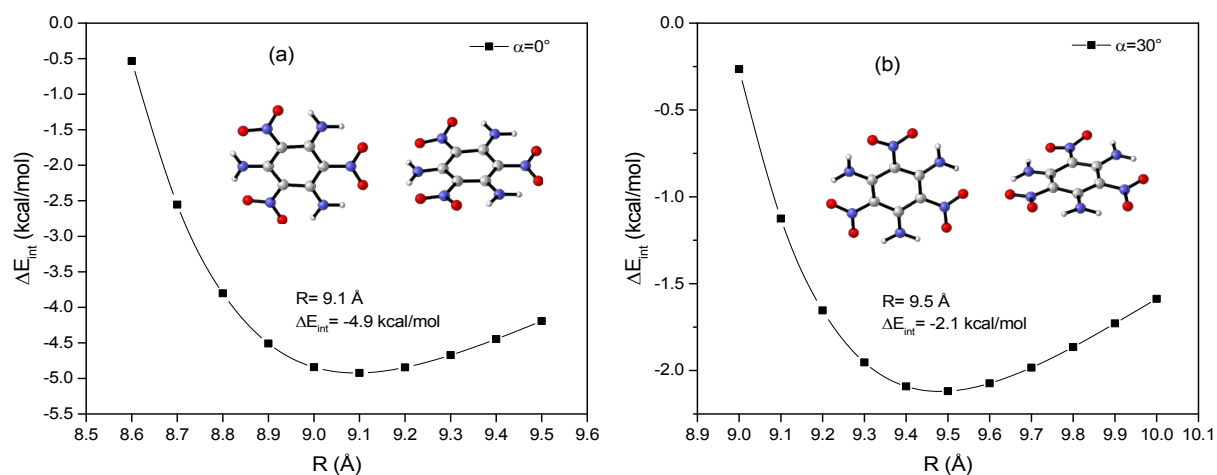


Figure S28. PESs of the crossing TATB dimers along (a) $\text{NH}_2\cdots\text{NO}_2$ and (b) $\text{NH}\cdots\text{NO}$.

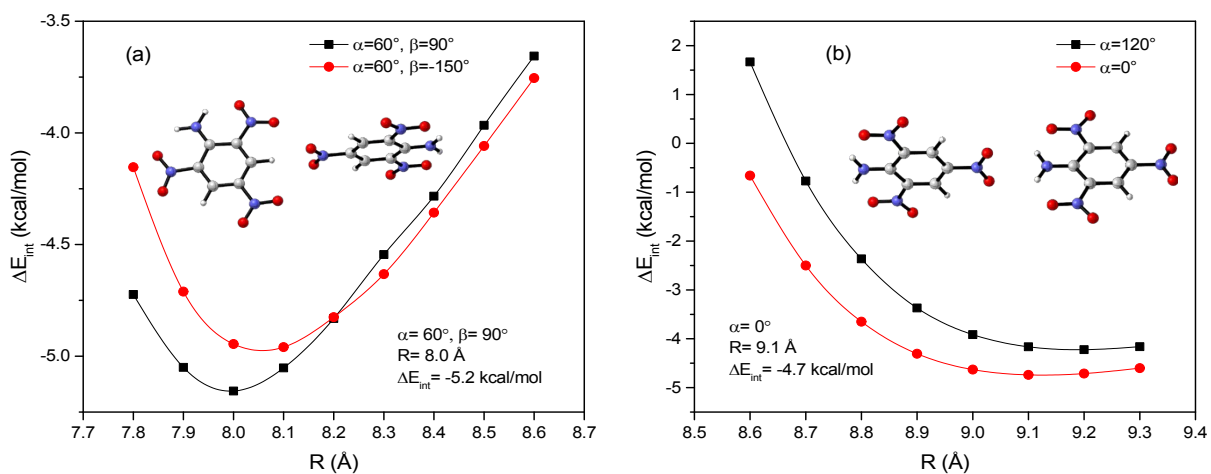


Figure S29. PESs of the crossing TNA dimers along (a) CH...NO₂ and (b) NH₂...NO₂.

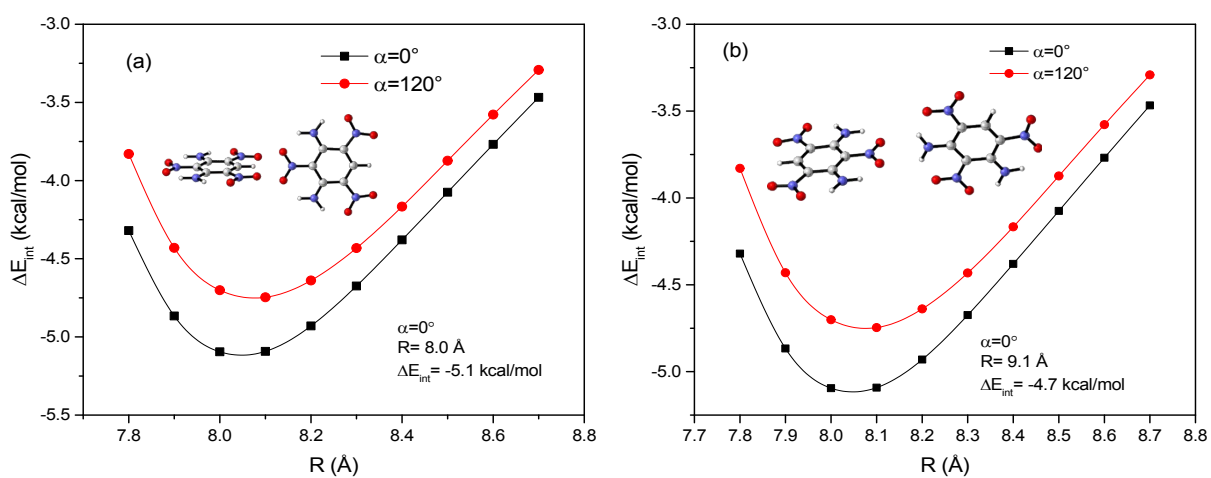


Figure S30. PESs of the crossing DATB dimers stacked along (a) CH...NO₂ and (b) NH₂...NO₂.

S6: Summary of the locally lowest points on all PESs and the related ΔE_{int} .**Table S1. Summary of the Locally Lowest Points on All PESs and the Related ΔE_{int} .**

No.	Label	α (°)	β (°)	φ (°)	θ (°)	γ (°)	R (Å)	ΔE_{int} (kcal/mol)
1	TNB-C1	0	0	90	0	0	8.8	-1.7
2	TNB-C2	40	60	90	0	0	7.9	-3.7
3	TNB-P1	15	30	50	0	0	4.9	-8.7
4	TNB-P2	285	30	40	0	0	4.3	-8.2
5	TNB-P3	105	30	50	0	0	4.9	-8.8
6	TNB-P4	0	30	0	0	0	3.6	-6.6
7	TNB-T1	0	0	0	90	0	6.5	-6.1
8	TNB-T2	0	0	0	90	30	6.6	-6.0
9	TNB-T3	0	180	0	90	0	5.5	-6.2
10	TNB-T4	0	180	0	90	30	5.5	-6.1
11	TNB-X1	0	30	90	90	90	8	-5.2
12	TNB-X2	40	20	90	90	130	7.8	-3.4
13	TATB-C1	0	0	90	0	0	9.1	-6.4
14	TATB-C2	32	60	90	0	0	8.9	-6.8
15	TATB-P	0	60	0	0	0	3.4	-18.2
16	TATB-T1	0	0	0	90	0	6.5	-7.7
17	TATB-T2	0	0	0	90	30	6.5	-7.8
18	TATB-T3	0	180	0	90	0	5.9	-6.5
19	TATB-T4	0	180	0	90	30	6	-6.0
20	TATB-X1	0	30	90	90	90	9.1	-4.9
21	TATB-X2	30	0	90	90	120	9.5	-2.1
22	TNA-C1	0	0	90	0	0	9	-6.1
23	TNA-C2	120	120	90	0	0	9.1	-5.6
24	TNA-C3	150	180	90	0	0	9	-6.9
25	TNA-P1	38	75	20	0	0	3.5	-11.7
26	TNA-P2	128	75	20	0	0	3.5	-12.7
27	TNA-P3	308	75	30	0	0	3.8	-10.6
28	TNA-P4	83	165	20	0	0	3.5	-12.6
29	TNA-P5	173	165	10	0	0	3.4	-11.2
30	TNA-P6	353	165	30	0	0	3.7	-12.6
31	TNA-PV1	0	75	0	0	0	3.4	-10.4
32	TNA-PV2	0	165	0	0	0	3.4	-10.8
33	TNA-T1	0	0	0	90	90	6.5	-7.0
34	TNA-T2	0	60	0	90	60	5.5	-7.6
35	TNA-T3	0	60	0	90	-60	5.5	-7.3
36	TNA-T4	0	120	0	90	90	6.5	-6.8
37	TNA-T5	0	120	0	90	-90	6.5	-6.3
38	TNA-T6	0	180	0	90	90	6	-4.2
39	TNA-X1	60	210	90	90	150	8.1	-5.0

40	TNA-X2	60	90	90	90	150	8	-5.2
41	TNA-X3	120	270	90	90	210	9.2	-4.2
42	TNA-X4	0	270	90	90	90	9.1	-4.7
43	DATB-C1	0	120	90	0	0	9.1	-6.5
44	DATB-C2	120	0	90	0	0	9.1	-5.9
45	DATB-C3	120	240	90	0	0	9.1	-5.8
46	DATB-C4	30	180	90	0	0	9.1	-6.6
47	DATB-C5	30	300	90	0	0	9	-7.0
48	DATB-C6	90	180	90	0	0	9	-7.2
49	DATB-P1	30	60	10	0	0	3.4	-15.3
50	DATB-P2	120	60	20	0	0	3.4	-16.1
51	DATB-P3	90	180	0	0	0	3.3	-15.2
52	DATB-P4	0	180	20	0	0	3.4	-16.2
53	DATB-PV1	0	60	0	0	0	3.3	-15.2
54	DATB-PV2	0	180	0	0	0	3.3	-15.2
55	DATB-T1	0	0	0	90	0	6.5	-7.3
56	DATB-T2	0	60	0	90	0	5.9	-5.9
57	DATB-T3	0	120	0	90	30	6.5	-7.3
58	DATB-T4	0	180	0	90	0	5.6	-8.7
59	DATB-X1	120	270	90	90	210	8.1	-4.7
60	DATB-X2	0	270	90	90	90	8	-5.1
61	DATB-X3	120	30	90	90	210	9.2	-4.6
62	DATB-X4	0	30	90	90	90	9.1	-4.7
